Sweetpotato root development influences susceptibility to black rot caused by the fungal pathogen *Ceratocystis fimbriata*

C. H. Parada-Rojas[1], Kenneth Pecota[2], C. Almeyda[3], G. Craig Yencho[2], and L. M. Quesada-Ocampo[1]*

[1]Department of Entomology and Plant Pathology, North Carolina State University, Raleigh, NC 27695, USA.

[2]Department of Horticulture, North Carolina State University, Raleigh, NC 27695-7616.

[3]Micropropagation and Repository Unit, North Carolina State University, Raleigh, NC 27695.

*Corresponding author: L. M. Quesada-Ocampo, E-mail: lmquesad@ncsu.edu

Key words: Ontogenic disease resistance, *Ceratocystis fimbriata*, sweetpotato, integrated disease management.

ORCID of authors:

C. H. Parada-Rojas: 0000-0002-8372-6012

Kenneth Pecota

C. Almeyda

G. Craig Yencho: 0000-0001-6583-0628

L. M. Quesada-Ocampo: 0000-0002-9072-7531

Camilo H. Parada-Rojas et al. *Phytopathology* 2

ABSTRACT

Black rot of sweetpotato caused by *Ceratocystis fimbriata*, is an important reemerging disease threatening sweetpotato production in the United States. This study assessed disease susceptibility of the storage root surface, storage root cambium, and slips (vine cuttings) of 48 sweetpotato cultivars, advanced breeding lines, and wild relative accessions. We also characterized the effect of storage root development on susceptibility to *C. fimbriata*. None of the cultivars examined at the storage root level were resistant, with most cultivars exhibiting similar levels of susceptibility. In storage roots, Jewel and Covington were the least susceptible and significantly different from White Bonita, the most susceptible cultivar. In the slip, significant differences in disease incidence were observed for above and below ground plant structures among cultivars, advanced breeding lines, and wild relative accessions. Burgundy and *Ipomoea littoralis* displayed less below ground disease incidence as compared to NASPOT 8, Sunnyside and LSU-417, the most susceptible cultivars. Correlation of black rot susceptibility between storage roots and slips was not significant, suggesting that slip assays are not useful to predict resistance in storage roots. Immature, early developing storage roots were comparatively more susceptible than older, fully developed storage roots. The high significant correlation between storage root cross-section area and cross-sectional lesion ratio suggests the presence of an unfavorable environment for *C. fimbriata* as the storage root develops. Incorporating applications of effective fungicides at transplanting and during early storage root development when sweetpotato tissues are most susceptible to black rot infection may improve disease management efforts.

INTRODUCTION

A Latin American vine, sweetpotato (*Ipomoea batatas* (L.) Lam) remains one of the most important food crops worldwide based on its estimated global production of 106 million tons (FAOSTAT 2017a). Sweetpotatoes are cultivated on about 9.2 million hectares of which 53% are grown in low income, food deficit countries (FAOSTAT 2017b). Sweetpotato storage roots are a valuable source of carbohydrates, fibers, iron, vitamin A, C, and some of the B-complex vitamins (USDA 2017). Orange fleshed sweetpotato cultivars contain *ß*-carotene, the precursor of vitamin A, which makes them desirable as a food source in sub-Saharan Africa; where vitamin A deficiency contributes to high rates of blindness, disease, and premature death in children and pregnant women (Sheikha and Ray 2015). The United States (US) currently ranks 10th in global annual production of sweetpotato (FAOSTAT 2017a). Value-added products such as sweetpotato fries and chips, as well as awareness of the nutritional benefits of the crop has led to an increase in sweetpotato consumption in the US and Europe (Scruggs and Quesada-Ocampo 2016b). Sweetpotatoes are considered a "high risk" crop due to the potential for weather related crop failures, and the aesthetic qualities of the crop that are often negatively affected by insect feeding and disease incidence (USDA 2018; Baselga et al. 2020; Stahr et al. 2020). North Carolina (NC) leads US sweetpotato production and in 2019 the state harvested more than 39,537 hectares with production valued at 323 million dollars (USDA-NASS 2019). Every year, sweetpotato production is limited by different abiotic and biotic factors, among which plant pathogens are a major threat to the industry. A few of the most notable sweetpotato plant pathogens include, *Fusarium solani* (Fusarium root rot), *Monilochaetes infuscans* (Sweetpotato scurf), *Streptomyces ipomoeae* (Streptomyces soil rot), *Macrophomina phaseolina* (Charcoal rot), *Rhizopus stolonifer* (Rhizopus soft rot), *Meloidogyne incognita* (Root-knot nematode), *Meloidogyne enterolobii*

(Guava root-knot nematode), and the recently re-emerging soilborne pathogen *Ceratocystis fimbriata*, the causal agent of black rot (Clark et al. 2013; Scruggs and Quesada-Ocampo 2016a; Scruggs et al. 2017).

Ceratocystis fimbriata causes serious infections on a wide range of plants worldwide, including cacao, coffee, coconut, sunn hemp, sycamore, poplar, almond, oak, taro, mango, and fig among others (Stahr and Quesada-Ocampo 2019). In sweetpotato, under favorable conditions the infection results in black, sunken cankers on sprouts or the developing roots, leading to stunting, wilting, chlorosis, and eventually death. Storage conditions post-harvest favor the development of black, firm lesions on the root surface often producing a sweet, fruity odor (M. Stahr and Quesada-Ocampo 2020). The center of the lesions is covered in perithecia and sticky ascospores that serve as pathogen propagules and aid in dissemination, contaminating equipment and leading to severe losses (Madison Stahr and Quesada-Ocampo 2020).

Historically, black rot was effectively controlled by cutting transplants above the soil line, using thiabendazole fungicides on seed roots, reducing wounds during harvest, properly curing roots, and sanitizing packing equipment (Clark and Moyer 1988). The implementation of integrated control strategies led to a drastic reduction in disease incidence in the US (Clark et al. 2013). Despite the continued implementation of these strategies, in 2015, black rot re-emerged as a significant threat for the sweetpotato industry in the US and Canada (Scruggs et al. 2017). The 2015 outbreak prompted the approval of a crisis emergency section 18 label for using thiabendazole postharvest on sweetpotato in North Carolina by the US Environmental Protection Agency (Quesada-Ocampo 2016). Nonetheless, fungicide use is becoming limited due to changes in maximum residue levels allowed for sweetpotato in international markets (USDA 2016).

Deployment of host resistance represents a desirable tool to ameliorate crop losses due to plant pathogens (Michelmore et al. 2017). However, breeding sweetpotato for disease resistance in combination with high yield and aesthetic traits, has been challenging due to the few breeding programs currently active in the US and the limited knowledge of the genetic basis of disease resistance in sweetpotato. Screening of sweetpotato cultivated lines in the 1950's identified highly resistant cultivars against black rot (Cheo 1953; Hildebrand 1957). However, descriptions of black rot resistance and screening ceased after 1962, but with the 2015 outbreak, interest in screening breeding lines for black rot resistance has regained importance (Scruggs et al. 2017; Wehner and LaBonte 2020). Currently, there is a need for robust phenotyping assays that allow rapid screening of sweetpotato accessions and wild relatives for resistance to black rot; nonetheless, many wild relatives are unable to produce storage roots. When assessing 14 common sweetpotato accessions and advanced breeding lines, Scruggs et al. (2017) employed a storage root wounding method and reported uniform susceptible phenotypes among accessions. However, lesion diameter measurements may ignore any level of resistance present in the storage root cambium, or at the slip level.

Developmental changes such as exponential growth of plant organs can result in higher or lower susceptibility to pathogens (Hu and Yang 2019). This phenomenon is known as ontogenic, developmental or age-related resistance. Multiple examples of developmental changes influencing levels of susceptibility exist on a wide range of crops including strawberry, grapes, pepper, rice, wheat, and cucumbers among others (Asalf et al. 2014; Gee et al. 2008; Kim et al. 1989; Zhao et al. 2009; Zhang et al. 2012; Mansfeld et al. 2020). In sweetpotato, several factors influence storage root growth including soil fertility, seasonality, and physiological changes in the storage roots (Dong et al. 2019). Expansion of storage root cambium cells during

development represents an important factor in sweetpotato root sizing that correlates strongly with age (Khan et al. 2016). Therefore, the aims of this study were to: 1) assess resistance in the storage root surface, storage root cambium, and slips of sweetpotato accessions and wild relatives; 2) determine if resistance in the storage root correlates with resistance in the slip; and 3) characterize the effect of storage root development on susceptibility to *C. fimbriata*. As wild relatives of sweetpotato could become a source of resistance, a slip screening assay may provide an effective and quick assessment of resistance to black rot for development of improved commercial varieties.

MATERIALS AND METHODS

Plant and fungal material

Accessions of *Ipomoea* species used in this study were obtained from the sources listed in Table 1. Among the accessions tested, we included 23 commercial lines, 14 African accessions, and 8 historical accessions of *I. batatas* as well as 3 wild *Ipomoea* species accessions. Virus indexed source plants were maintained in the greenhouse under a 16 h-light/8 h-dark photoperiod and grown in 15-cm pots filled with peat moss-vermiculite potting media (Conrad Fafard Inc., Agawam, MA). Plants were watered twice daily and fertilized with 20N–10P–20K weekly. Mother plants were propagated into 72-cell trays filled with the same potting media as described above to obtain slips (vine cuttings) needed for black rot slip experiments. Additionally, to assess susceptibility to black rot in the storage root, roots from 16 commercial lines were utilized. Storage roots from commercial and advanced breeding lines were obtained from the Sweetpotato Breeding and Genetics Program at NC State University and from individual commercial sweetpotato farms without a history of *C. fimbriata*. Covington sweetpotato storage roots at

different developmental stages were also obtained from the Sweetpotato Breeding and Genetics

Program ensuring that all roots originated from the same clone. Fungal isolate AS236 was used

to compare the different disease phenotyping methods, as this isolate was previously reported

highly virulent against several cultivars of sweetpotato (Scruggs et al. 2017). Fungal cultures

were maintained at 21 ± 2 °C under continuous fluorescent light. Agar plugs (5-mm diam) from

the margins of actively growing colonies were transferred to new autoclaved carrot juice agar (16

g agar, 160 ml unfiltered carrot juice, and 840 ml distilled water) and maintained under the

conditions indicated above.

Inoculum preparation

Ascospores from actively growing cultures of isolate AS236 were plated onto new carrot

agar plates and allowed to grow for 2 weeks. Ascospores were collected using an L-shaped glass

rod to scrape sticky ascospores from fungal cultures. The ascospores were suspended in 5 ml of

distilled water with a drop of Tween 20 solution. This suspension was vortexed at low speed for

1 min to allow spore masses to separate. Hat shaped ascospores were quantified using a

hemocytometer and the suspension was used at a concentration of 10^3 ascospores/ml for both

storage root and slip inoculations.

Black rot susceptibility screening of *Ipomoea batatas* storage roots

Storage roots from 16 cultivars and advanced breeding lines were screened for resistance

to black rot. Inoculation was as described by Scruggs et al. (2017) using the isolate AS236. Six

storage roots per accession were wounded and inoculated with 10 µL of the ascospore

suspension or with sterile deionized water to serve as a non-inoculated control. The experiment

was a completely randomized design with six replicate storage roots per cultivar, per treatment (inoculated or control), and the experiment was repeated three times. Roots were placed individually into clear 28 cm × 20 cm × 14 cm plastic containers, each with a sterile paper towel dampened with 15 ml of sterile water to maintain high humidity as previously described by Scruggs and Quesada-Ocampo (2016b). Roots were incubated under dark conditions at approximately 23°C in a precision incubator model 30M (Thermo Scientific, Wilmington, DE) part of the NC State University Phytotron facility. Lesion diameters were recorded at 4, 8, 12, 16, 20, and 24 days post inoculation and the data was used to calculate area under disease progress curve (AUDPC) values for each root according to Madden et al. (2007). In addition, the cross-sectional lesion ratio (CLR) was measured at the end of the experiment using the image analysis software Fiji (Schindelin et al. 2012). To measure the CLR, roots were sliced at the center of the disease lesion producing a 1-2-cm thick slice. Each slice was placed flat and with the lesion facing up onto a black background surface for contrast. Two standardized metric rulers were placed to the left and above the root slice respectively to provide a reference for downstream image analysis (Fig. 1). Each root image was uploaded to Fiji and converted to an 8-bit grayscale. Pixels were converted to mm^2 by drawing a 50-mm line over a section of the reference metric rulers positioned in each photo. This process was repeated 30 times for each of the four repetitions to account for differences in camera angle and viewpoints. An automated threshold routine was established to obtain a binary image and highlight infected areas as black pixels. This routine was repeated to also highlight the total root cross-section area. The free hand tool was used to surround the infected lesion area and total root cross-section area, then, selected black pixels were recorded in mm^2. The CLR was calculated using the following equation:

$$CLR = \frac{Infected\ cross-section\ area\ (mm^2)}{Total\ root\ cross-section\ area\ (mm^2)} \tag{1}$$

Black rot susceptibility screening of *Ipomoea spp.* slips

Forty-seven sweetpotato cultivars, advanced breeding lines, and wild relative accessions were propagated in 72-cell trays to generate 40 slips per accession. Twenty centimeter long slips were cut following sweetpotato planting practices (Edmunds et al. 2008) and subsequently inoculated by dipping the bottom 4-cm of the stems into an ascospore suspension (10^3 ascospores/ml) for 10 min. Inoculated slips were transplanted into 11-cm-depth cone flats filled with peat moss-vermiculite potting media (Conrad Fafard Inc., Agawam, MA). Treatment blocks consisted of 10 slips from each accession that were placed in a row of 10 cells within a flat. Blocks were arranged in a completely randomized block design with four replications. Slips were grown for 42 days on a greenhouse under a 16 h-light/8 h-dark photoperiod, watered twice daily, and fertilized with 20N–10P–20K weekly. Incidence of above ground symptoms was recorded at 0, 9, 13, 17, 21, 25, 29, and 33 days post-inoculation. Root systems were washed and scored for incidence of black necrotic lesions at 42 days post-inoculation.

Effect of storage root development on susceptibility to black rot

Orange flesh cv. Covington sweetpotato clones were produced by the Sweetpotato Breeding and Genetics Program at NC State University. Briefly, Covington plants were grown at the Horticultural Crops Research Station in Clinton, NC, USA. Harvested storage roots were cured at 29°C, 85–90% relative humidity for 5 days and stored at 14–16°C, 85–95% relative humidity for 2 weeks before analysis. A total of 224 storage roots representing three commercial grades (Canners, US #1, and Jumbos) were selected for this experiment. Roots were placed randomly in plastic containers and inoculated with *C. fimbriata* isolate AS236 as described by

Scruggs et al. (2017). Roots serving as controls were wounded and 10 µL of sterile water pipetted onto the wound. Roots were incubated at 23°C in dark conditions. Twenty-four days post inoculation, surface lesion diameter was measured twice perpendicularly for each storage root. Total cross-section root area and infected cross-section area was measured using the image analysis described above. Total cross-sectional root area was used as a proxy for storage root development and age. This parameter is comparable to transverse diameter measurements described by Dong et al. (2019).

Data analysis

For both the storage root and slip screening assays, mixed model analyses were performed using PROC GLIMMIX in SAS v. 9.4 (SAS Institute Inc., Cary, NC) to examine the effects of cultivar on AUDPC, CLR, and above and below ground disease incidence values. For these response variables, cultivar was treated as a fixed effect and repetitions were treated as a random effect. The quantile plots for AUDPC met the assumptions of normality. However, CLR and above and below ground incidence did not meet the assumptions and therefore were analyzed using the gamma (CLR) and beta (above and below ground disease incidence) distributions. All means were separated using the Tukey-Kramer multiple comparison test ($\alpha = 0.05$) to determine the significance of mean differences among cultivars. In addition, we implemented the rank-sum classification method described by Afolabi et al. (2008) to obtain a combined rank for cultivars screened in the storage root assay. Deviations were color coded to denote the level of susceptibility with deviations close to -4 indicating lesser susceptibility and deviations close to +4 indicating greater susceptibility (Table 2). In order to determine correlation between slip and storage root assays, the storage root variables (AUDPC, CLR)

deviations calculated from the rank sum method and the below ground disease incidence were used to compute the Spearman's rho rank correlation coefficients and the asymptotic P-values in R Studio version 1.1.463 (R Studio, Inc. 2019) using the package *Hmisc* version 4.2-0.

For the storage root development experiment, surface lesion diameter at 24 dpi and CLR values for each root inoculated were used to evaluate the effect of total cross-sectional root area on susceptibility to *C. fimbriata*. The quantile plot for lesion diameter met the assumptions of normality. We tested the effect of total cross-sectional root area on surface lesion diameter using the *lmrob* function in the R package robustbase (R Core Team 2019). CLR values were not normally distributed justifying a nonparametric analysis using Spearman correlation method in the R package psych (Revelle 2017). Figures were generated using the ggplot2 R package (Wickham et al. 2013).

RESULTS

Isolate AS236 successfully caused infection during storage root and slip inoculations. Indicative black rot symptoms developed across all US cultivated and historical sweetpotato cultivars, African sweetpotato cultivars, and wild *Ipomoea* species (Fig. 1 and 3, and Supp. Fig. 1). Symptomatic storage roots displayed black circular surface lesions of approximately 3.0 cm in diameter and storage root cambium deterioration (Fig. 1 and 4). Similarly, symptomatic slips exhibited wilting, cracking of the stem, and black necrotic lesions in the crown or base of the slip (Fig. 3 and Supp. Fig. 1).

Black rot susceptibility screening of *Ipomoea batatas* storage roots

Storage roots of all 16 sweetpotato cultivars exhibited black rot symptoms by 4 dpi. Significant differences among the 16 sweetpotato cultivars were detected for both AUDPC ($P < 0.0001$) and CLR means ($P < 0.0001$). The severity of black rot lesions on the surface of roots measured as AUDPC values ranged from 23.44 to 33.77 (Table 2). The mean response of cultivars at the storage root cambium measured as CLRs ranged from 0.08 to 0.28 (Table 2). Out of the 16 cultivars screened for AUDPC, only Jewel and Covington displayed significantly lower AUDPC values when compared to the most susceptible cultivars Hatteras, Bellevue, and White Bonita. Cultivars Jewel and Covington also exhibited significantly lower CLR values than those of White Bonita and Bellevue (Fig. 1). In addition, we observed smaller lesion diameters and stalled surface growth differences for both Jewel and Covington storage roots in the early days post inoculation (Fig. 2). Cultivars Orleans, Bayou Belle, Porto Rico, Averre, Burgundy, and Stokes Purple exhibited higher AUDPC values but were not significantly different from Hatteras (Table 2). Similarly, cultivars Porto Rico and Stokes Purple showed high CLR values but were not significantly different from White Bonita. Cultivar Stokes Purple, the only purple flesh sweetpotato included in this study, exhibited equivalent values of AUDPC and CLRs and was not significantly different from Hatteras or White Bonita. Considering the response of cultivars to black rot infections in the surface (AUDPC) and cambium (CLR) of the storage roots when classifying cultivars based on disease susceptibility, we employed the rank sum method of classification which ranked both variables and produced deviations from the grand mean of ranks allowing for comparisons across all 16 cultivars. As denoted in Table 2, cultivars Jewel (-3.68) and Covington (-3.68) displayed the largest negative deviations among cultivars and could be therefore classified as moderately susceptible. The Spearman rank correlation coefficient showed a non-significant weak positive correlation ($\rho = 0.33$, $P = 0.2149$) between AUDPC (surface) and

CLR (cambium) values. Despite the lack of significant correlation, several of the cultivars with the lowest AUDPC values had comparatively lower CLR values. Therefore, we consider the rank sum method and deviations from the grand mean more informative for phenotyping sweetpotato susceptibility to black rot.

Black rot susceptibility screening of *Ipomoea spp.* slips

Slips of all *Ipomoea* spp. accessions tested exhibited below ground black rot symptoms. Above ground symptoms first became visible at 9 dpi (Supp. Fig. 1). Significant differences among 47 sweetpotato cultivars, advanced breeding lines, and wild relative accessions were detected for both above ($P < 0.0001$) and below ground disease incidence means ($P < 0.0001$) (Table 3). Above ground disease incidence ranged from 1.73 to 72.53 while below ground disease incidence ranged from 22.90 to 97.50 (Table 3). We observed large variation in the above ground disease incidence means, however, two main groups emerged from the Tukey-Kramer test comparison. The first one included *I. trifida*, New Kawogo, *I. triloba*, Ejumula, Travis, and NASPOT 8. Cultivars in the first group exhibited significantly higher above ground disease incidence compared to the second group which was comprised of NASPOT 10 O, Japanese, Bwanjule, O'Henry, Covington, Dimbuka Bukulula, Chuanshu 27, Apache, Hopi, NC-413, White Bonita, Norin 2, Bellevue, NC04531, NASPOT 4, VitA NASPOT 9 O, Orleans, Kabode, Beauregard, Mahon, Burgundy, Norton, Jewel, and Hernandez. From all cultivars screened for differences in above ground disease incidence, Beauregard, Mahon, Burgundy, Norton, Jewel, and Hernandez displayed significantly lower means when compared to the most susceptible cultivar *I. trifida*. The majority of cultivars assessed for below ground disease incidence grouped together in two major sets according to the Tukey-Kramer test comparison

(Table 3). The first set comprised Travis, NSP306, Ejumula, NASPOT 9 O, Bayou Belle, Tomulabula, New Kawogo, Hopi, Carolina Ruby, White Bonita, Porto Rico, Japanese, and Bellevue which exhibited no significant differences for below ground disease incidence when compared to Naspot 8, Sunnyside, and LSU-417 (highly susceptible). For the second set, below ground disease incidence means of Stokes Purple, Chuanshu 27, Norin No.2, Bwanjule, NASPOT 5, Mahon, NCNSP0323, Kakamega 45879, Averre, Tanzania, NASPOT 10 O, NC04531, O'Henry, Kabode, AllGold, Norin No.4, NASPOT 4, Jishu5, Jewel, Murasaki, Evangeline, Norton, Apache, Dimbuka Bukulula, Beauregard, Covington, Hernandez, VitA NASPOT 9 O, Orleans, and *I. littoralis* were not significantly different from Burgundy (highly resistant). In contrast with the storage root phenotypes observed for cultivar Burgundy, during the slip assay Burgundy had the lowest below ground disease incidence (22.90) compared with NASPOT 8 (97.50), Sunnyside (97.50), and LSU-417 (97.50) (Figure 3). Burgundy displayed lower below ground disease incidence than NASPOT 8, however, Burgundy was not significantly different from Naspot 8 for above ground disease incidence. *I. trifida*, a wild relative of *I. batatas*, exhibited higher below ground disease incidence than *I. littoralis*, one of the only *Ipomoea* species not endemic to the Americas. We calculated the Spearman rank correlation coefficient to determine correlation of above and below ground disease incidence. This resulted in a non-significant weak positive correlation ($\rho = 0.28$, $P = 0.0606$) with many cultivars being asymptomatic above ground but exhibiting higher below ground disease incidence. Because of this weak correlation, we selected below ground disease incidence as the most informative factor to compare against storage roots.

Fifteen sweetpotato cultivars were assessed for both storage root and slip resistance to black rot. We used the Spearman rank correlation coefficient to determine the association

between deviations from the grand mean obtained from the rank sum method for storage roots (AUDPC and CLR) and below ground disease incidence for slips. Interestingly, the association was moderate and non-significant ($\rho = 0.48$, $P = 0.0685$) suggesting differential tissue dependent resistance. Cultivars with larger negative deviations such as Covington and Jewel displayed 40.90 and 53.90 below ground disease incidence, respectively. Burgundy ranked poorly in the storage root assay but displayed significantly lower below ground incidence. This phenomenon can be visualized by comparing Burgundy in Figures 1 and 3.

Effect of storage root development on susceptibility to black rot

Inoculated Covington storage roots became diseased in all roots tested, confirming the viability of inoculum and storage conditions for infection. Roots treated with sterile water remained asymptomatic with wounds desiccating but without displaying visible changes in the storage root core. To assess the effect of storage root development on black rot susceptibility, we defined the storage root cross-sectional area as representative of age. Roots of all sizes exhibited differences in their susceptibility to black rot that appeared to be influenced by the total cross-sectional root area, with a discernible pattern for greater flesh susceptibility in smaller roots (Fig. 4). Total cross-sectional root area ranged between 735.11 mm^2 and 9873.30 mm^2. Surface lesion diameter at 24 dpi varied between 0.95 cm to 3.20 cm while CLR values fluctuated between 0.01 and 0.37. Surface lesion diameter had independent values from the total cross-sectional root area (Fig. 2S), and linear regression analysis revealed a weak and non-significant correlation between surface lesion diameter and total cross-sectional root area ($R^2 = 0.01$; $P = 0.105$). In contrast, CLR values decreased drastically at total cross-sectional root areas greater than 4000 mm^2 (Fig.

5). We observed a strong significant negative correlation between CLR values and total cross-sectional root area (Spearman's r = -0.77; P < 0.0001).

DISCUSSION

Our storage root screening assay revealed that cultivars Jewel and Covington are less susceptible to *C. fimbriata* isolate AS236 compared to other tested genotypes. However, despite that AUDPC and CLR means for both cultivars were less than those of White Bonita, we observed significant fungal growth and lesions that would make roots unmarketable if infected. Due to their disease susceptibility, strategies other than host resistance need to be implemented for black rot management when using Jewel and Covington roots for sweetpotato production. Scruggs et al. (2017) identified comparably low AUDPC values for Covington when examining resistance to the same isolate of *C. fimbriata* utilized in this study. Similarly, Scruggs and colleagues were unable to classify Covington as resistant to *C. fimbriata* on the basis of storage root surface lesion diameter. In fact, to our knowledge resistance to *C. fimbriata* at the storage root level remains unknown. Lack of resistance in current US sweetpotato cultivars may be explained by the fact that this trait has not been a priority for breeding programs since the 1950s (Cheo 1953; Hildebrand 1957; Clark et al. 2013).

Our method to assess resistance at the storage root level was inspired by the work of Hildebrand (1957) when he assessed 300 sweetpotato cultivars and breeding lines for resistance to *C. fimbriata* in the US. His description of cross-sectional area of lesions caused by *C. fimbriata* led us to supplement our surface lesion measurements with the cross-sectional lesion ratio in current sweetpotato cultivars. We found that infections in the surface of the sweetpotato storage root correlated weakly with CLR values, contradicting Hildebrand (1957) findings, who

reported a correlation coefficient of 0.745 between lesion diameter and cross-sectional area of lesion. However, assessing the internal tissue of storage roots provided a robust and objective method for evaluating the response of cells beyond the epidermis of the sweetpotato storage root. Storage root formation begins with the development of a cork cambia around the secondary xylem element on the underground nodes of transplanted slips (Tanaka 2016; Khan et al. 2016; Tonn and Greb 2017). Covington and Jewel exhibited constrained fungal growth as the lesion progresses into the storage root core suggesting some components of the newly forming cambium create an unfavorable environment for *C. fimbriata*. Weimer and Harter (1921) likewise reported the inability for *Rhizopus tritici* to penetrate the cork cambium of sweetpotato. In the vegetatively propagated root crop, cassava, the cambium of oomycete root rot resistant genotypes exhibited thicker cells than those of the susceptible genotypes (Silva et al. 2017). Also, Araujo et al. (2014) found that *C. fimbriata* hyphae grew unconstrained in the xylem elements of susceptible mango cultivars, while in resistant cultivars the fungus never penetrated the cork cambium. Screening the cross-section of storage roots may reveal potential resistance at different layers of the sweetpotato root core. Moyer et al. (1984) examined both fibrous roots and storage root slices for resistance to *S. ipomoea* and described unexpected resistance in the root core as compared to other parts of the sweetpotato. Despite weak correlations between CLR and AUDPC in our study, a pattern of susceptibility emerged among the 16 sweetpotato cultivars. We considered both CLR and AUDPC mean values to provide a comprehensive ranking that facilitates interpretation of the susceptibility response. This rank classification was used in other root crops like cassava and to discover sources of resistance in maize (Afolabi et al. 2008; Ariyo et al. 2010).

To determine if resistance at the storage root level correlates with resistance at the slip level, we developed an assay that would allow for rapid screening of both commercial cultivars as well as wild relatives of sweetpotato that do not produce storage roots (Nimmakayala et al. 2011; Wu et al. 2018). Based on the assessment of 47 sweetpotato cultivars, advanced breeding lines, and wild relative accessions**,** this study underscored key differences between foliage and root symptoms as below ground incidence contradicted above ground ratings for some cultivars. During the time span of this experiment, crowns for many of the cultivars developed black necrotic lesions, produced roots above the lesions, and mostly appeared asymptomatic above ground. Root formation above the inoculation site has been documented on tomatoes (Quesada-Ocampo and Hausbeck 2010), peppers (Dunn and Smart 2015), and maize (Quesada-Ocampo et al. 2016) when inoculating with vascular pathogens. The asymptomatic foliage may result in large scale crop losses that are only realized at harvest or more likely post-harvest once roots are washed and black rot lesions are visible (Clark et al. 2013; Quesada-Ocampo 2018). These findings highlight the importance of examining multiple tissues of the sweetpotato that are relevant to production practices when breeding for disease resistance.

The combined analysis of storage root surface lesions, CLR, and slip below ground incidence allowed us to discover an underlying pattern of tissue dependent response to *C. fimbriata* in sweetpotato. Correlation of black rot resistance between storage roots and slips was not significant, suggesting that the slip assay is unable to predict resistance in the storage root. This relationship between sweetpotato storage roots and slips underscored the potential for a developmental stage, tissue age, or tissue type driving the response to infections with *C. fimbriata*; similar to the response to inoculations with *Phytophthora capsici* initially described in cucumbers of different size and age (Gevens et al. 2006). These observations lead us to examine

the effect of storage root cross-section area on susceptibility to *C. fimbriata*. Cross-sectional

lesion ratio (CLR) on Covington sweetpotato roots of different total cross-section area strongly

suggested a case of ontogenic resistance. We defined black rot ontogenic resistance in

sweetpotato roots as the decline of susceptibility to *C. fimbriata* during the development of

storage roots (Villordon et al. 2014). To our knowledge, this represents the first description of

this defense phenomena in sweetpotato. Economically important fruits, vegetables, and crops

exhibit ontogenic resistance to oomycete, fungal, and bacterial pathogens (Gusberti et al. 2013;

Asalf et al. 2014; Torres et al. 2017; Cui et al. 2018; Alzohairy et al. 2019). The underlying

mechanism of ontogenic resistance remains unclear for many pathosystems, however, growing

evidence suggests that a sophisticated intrinsic regulatory network coordinates defense responses

to pathogens during development (Hu and Yang 2019). Associated defense responses include

organ maturation, vegetative phase change, and floral transition (Hu and Yang 2019). In

sweetpotato, expansion of root diameter is accomplished by rounds of cell division, expansions

of primary cambium, and emergence of secondary cambium (Tanaka 2016). These structural

changes in storage roots coincide with upregulation of the *SRF6* gene in the primary and

secondary cambium of sweetpotato (Tanaka et al. 2005). *SRF6* is a homolog of the NSP-

interacting kinase (NIK) in *Arabidopsis*, which is involved in plant development and defense

signaling against geminivirus infection (Santos et al. 2010). We speculate that as primary and

secondary cambium develops, an unknown mechanism leads to an unfavorable environment for

C. fimbriata infection. Harter and Weimer (1929) documented a pattern of *C. fimbriata* growth

restriction in inoculated storage roots and attributed the lack of widespread infection to a layer of

cells developing below the cork cambium. Further research could explore the mechanism for

ontogenic resistance in sweetpotato to *C. fimbriata* by examining cytological changes in the storage root cambium cells.

We included a diverse panel of sweetpotato cultivars that spans both geographically and temporally with some sweetpotato cultivars sourced from Africa, Louisiana, North Carolina, and others archived in the United States Department of Agriculture Germplasm Repository from the 1950s. African cultivars were included in this study as breeding programs have developed mapping populations that could potentially aid in the characterization and segregation of resistance to black rot and other pathogens (Abidin et al. 2005; Gibson et al. 2008; Mwanga et al. 2011; David et al. 2018; Pereira et al. 2019). In this study, VitA NASPOT 9 O exhibited significant differences from Sunnyside and can be classified as moderately resistant at the slip level. However, further research needs to confirm the response at the storage root level. The three wild relatives that we included in the slip screening assay were endemic to the Americas except for *I. littoralis* which is native to Pacific and Indian ocean coast lines (Austin 1991). In our study, *I. trifida,* a diploid wild relative that serves as a reference for genome improvement studies of the hexaploid *I. batatas* (Wu et al. 2018), performed poorly and we classified it as susceptible to black rot. In contrast, *I. littoralis* displayed low below ground incidence and potentially could be a candidate for improving sweetpotato resistance to *C. fimbriata* (CIP 1988). In fact, in the 1980's Chinese researchers produced hybrid progenies between *I. batatas* and *I. littoralis* and documented higher levels of resistance to *C. fimbriata* in F1 hybrids than local Chinese sweetpotato cultivars (Holden et al. 1993). In the 1950s, Sunnyside was utilized as a resistant check to screen sweetpotatoes for susceptibility to black rot (Cheo 1953). Our study documented high levels of below ground incidence for Sunnyside and other cultivars from that period of time. Cheo's publication lacks details on ascospore concentrations and size of storage

roots tested. The discrepancy between our results and those of Cheo could be explained by the use of different *C. fimbriata* isolates, but the exact reason remains unclear. Regardless, our results suggest that current *C. fimbriata* populations have evolved to overcome any resistance present in Sunnyside (Cheo 1953). The use of ascospore suspensions of *C. fimbriata* isolate AS236 allowed for consistent and effective screening of a wide range of *I. batatas* and wild relatives germplasm in our current study and in Scruggs et al. (2017). Despite only utilizing a single isolate of *C. fimbriata*, the very high incidence of black rot lesions both at the root and slip level demonstrated that the isolate was highly virulent after repeated subculturing.

In summary, our experiments demonstrated that susceptibility to black rot is widespread among storage roots of cultivated sweetpotatoes. Both storage root and slip screenings led us to discover a strong decline in susceptibility on younger and newly developing storage roots. These findings have implications for management of black rot susceptible sweetpotato cultivars. Sweetpotato growers and packing houses commonly apply effective fungicides in seed beds and postharvest (Quesada-Ocampo 2016; Scruggs et al. 2017; Clark et al. 2013). However, according to our results, timely fungicide applications could protect slips and developing storage roots in fields with history of *C. fimbriata*. Further studies need to understand developmental factors involved in ontogenic resistance of sweetpotato and application time of fungicides to reduce risk of infections postharvest. The absence of complete resistance in storage roots for cultivated sweetpotatoes warrants further research to examine whether compatible wild relatives such as *I. littoralis* could be used to produce hybrid progenies with increased resistance to black rot. Breeding sweetpotatoes for resistance to plant pathogens like *C. fimbriata* remains a lower priority than breeding for yield and aesthetics of this crop, especially when chemical and cultural control strategies were efficacious. However, at this time chemical control strategies are banned

for use in many key markets for sweetpotato such as the European Union, which severely limits the ability of US growers to control black rot. Thus, host resistance remains a key element for integrated disease management of black rot and requires further investigation.

ACKNOWLEDGEMENTS

LITERATURE CITED

Abidin, P. E., Eeuwijk, F. A. van, Stam, P., Struik, P. C., Malosetti, M., Mwanga, R. O. M., et al. 2005. Adaptation and stability analysis of sweet potato varieties for low-input systems in Uganda. Plant Breed. 124:491–497.

Afolabi, C. G., Ojiambo, P. S., Ekpo, E. J. A., Menkir, A., and Bandyopadhyay, R. 2008. Novel sources of resistance to Fusarium stalk rot of maize in tropical Africa. Plant Dis. 92:772–780.

Alzohairy, S. A., Hammerschmidt, R., and Hausbeck, M. K. 2019. Changes in Winter Squash Fruit Exocarp Structure Associated with Age-Related Resistance to *Phytophthora capsici*. Phytopathology. 110:447–455.

Araujo, L., Bispo, W. M. S., Cacique, I. S., Cruz, M. F. A., and Rodrigues, F. A. 2014. Histopathological aspects of mango resistance to the infection process of *Ceratocystis fimbriata*.

Plant Pathol. 63:1282–1295.

Ariyo, O., Dixon, A., and Atiri, G. 2010. The Relative Resistance of Cassava Cultivars to African Cassava Mosaic Disease (ACMD) as Determined by Two Methods: Rank-Sum and the Area Under the Disease Progress Curve. Arch. Phytopathol. Plant Prot. 35:23–30.

Asalf, B., Gadoury, D. M., Tronsmo, A. M., Seem, R. C., Dobson, A., Peres, N. A., et al. 2014. Ontogenic Resistance of Leaves and Fruit, and How Leaf Folding Influences the Distribution of Powdery Mildew on Strawberry Plants Colonized by *Podosphaera aphanis*. Phytopathology. 104:954–963.

Austin, D. F. 1991. *Ipomoea littoralis* (Convolvulaceae)—taxonomy, distribution, and ethnobotany. Econ. Bot. 45:251–256.

Baselga, F. M. de E., Schultheis, J. R., Boyette, M. D., Quesada-Ocampo, L. M., Starke, K. D., and Monks, D. W. 2020. Vine Removal Prior to Harvest, and Curing Duration and Temperature Affect the Incidence and Severity of Internal Necrosis in 'Covington' Sweetpotato. HortTechnology. 30:544–551.

Cheo, P. C. 1953. Varietal differences in susceptibility of sweet potato black rot fungus. Phytopathology. 43:78–81.

CIP. 1988. *Exploration, Maintenance, and Utilization of Sweet Potato Genetic Resources: Report of the First Sweet Potato Planning Conference, 1987*. International Potato Center.

Clark, C. A., Ferrin, D. M., Smith, T. P., and Holmes, G. J. 2013. *Compendium of sweetpotato diseases, pests, and disorders*. St. Paul, MN: American Phytopathological Society.

Clark, C. A., and Moyer, J. W. 1988. *Compendium of sweet potato diseases*. St. Paul, MN: American Phytopathological Society.

Cui, M., Wang, C., Zhang, W., Pervaiz, T., Haider, M. S., Tang, W., et al. 2018. Characterization of Vv-miR156: Vv-SPL pairs involved in the modulation of grape berry development and ripening. Mol. Genet. Genomics. 293:1333–1354.

David, M. C., Diaz, F. C., Mwanga, R. O. M., Tumwegamire, S., Mansilla, R. C., and Grüneberg, W. J. 2018. Gene Pool Subdivision of East African Sweetpotato Parental Material. Crop Sci. 58:2302–2314.

Dong, T., Zhu, M., Yu, J., Han, R., Tang, C., Xu, T., et al. 2019. RNA-Seq and iTRAQ reveal multiple pathways involved in storage root formation and development in sweet potato (*Ipomoea batatas* L.). BMC Plant Biol. 19:136.

Dunn, A. R., and Smart, C. D. 2015. Interactions of *Phytophthora capsici* with Resistant and Susceptible Pepper Roots and Stems. Phytopathology. 105:1355–1361.

Edmunds, B., Boyette, M., Clark, C. A., Ferrin, D. M., Smith, T. P., and Holmes, G. J. 2008. *Postharvest Handeling of Sweetpotatoes*. Zebulon, NC: North Carolina Cooperative.

FAOSTAT. 2017a. Global sweetpotato production and area harvested. Available at: http://www.fao.org/faostat/en/#search/Sweet%20potatoes.

FAOSTAT. 2017b. Low-Income Food-Deficit Countries (LIFDCs) - List for 2018. Available at: http://www.fao.org/countryprofiles/lifdc/en/.

Gee, C. T., Gadoury, D. M., and Cadle-Davidson, L. 2008. Ontogenic Resistance to *Uncinula necator* Varies by Genotype and Tissue Type in a Diverse Collection of *Vitis* spp. Plant Dis. 92:1067–1073.

Gevens, A. J., Ando, K., Lamour, K. H., Grumet, R., and Hausbeck, M. K. 2006. A Detached Cucumber Fruit Method to Screen for Resistance to *Phytophthora capsici* and Effect of Fruit Age on Susceptibility to Infection. Plant Dis. 90:1276–1282.

Gibson, R. W., Byamukama, E., Mpembe, I., Kayongo, J., and Mwanga, R. O. M. 2008. Working with farmer groups in Uganda to develop new sweet potato cultivars: decentralisation and building on traditional approaches. Euphytica. 159:217–228.

Gusberti, M., Gessler, C., and Broggini, G. A. L. 2013. RNA-Seq Analysis Reveals Candidate Genes for Ontogenic Resistance in Malus-Venturia Pathosystem. PLOS ONE. 8:e78457.

Harter, L. L., and Weimer, J. 1929. *A monographic study of sweet-potato diseases and their control*. United States Department of Agriculture.

Hildebrand, E. M. 1957. Testing sweet potatoes for black rot resistance. Plant Dis. Report. 41:661–670.

Holden, J., Peacock, W. J., Peacock, J., and Williams, T. 1993. *Genes, Crops and the Environment*. Cambridge University Press.

Hu, L., and Yang, L. 2019. Time to Fight: Molecular Mechanisms of Age-Related Resistance. Phytopathology. 109:1500–1508.

Khan, M. A., Gemenet, D. C., and Villordon, A. 2016. Root System Architecture and Abiotic Stress Tolerance: Current Knowledge in Root and Tuber Crops. Front. Plant Sci. 7:1584.

Kim, Y., Hwang, B., and Park, K. 1989. Expression of Age-Related Resistance in Pepper Plants Infected with *Phytophthora capsici*. Plant Dis. 73:745–747.

Madden, L. V., Hughes, G., and Bosch, V. F. 2007. *The Study of Plant Disease Epidemics*. St. Paul, MN.: American Phytopathological Society.

Mansfeld, B. N., Colle, M., Zhang, C., Lin, Y.-C., and Grumet, R. 2020. Developmentally regulated activation of defense allows for rapid inhibition of infection in age-related resistance to *Phytophthora capsici* in cucumber fruit. BMC Genomics. 21:628.

Michelmore, R. W., Coaker, G., Bart, R., Beattie, G. A., Bent, A., Bruce, T., et al. 2017. Foundational and translational research opportunities to improve plant health. Mol. Plant. Microbe Interact. 30:515–516.

Moyer, J. W., Campbell, C. L., Echandi, E., and Collins, W. W. 1984. Improved Methodology for Evaluating Resistance in Sweet Potato to *Streptomyces ipomoea*. Phytopathology. 74:494–497.

Mwanga, R. O. M., Niringiye, C., Alajo, A., Kigozi, B., Namukula, J., Mpembe, I., et al. 2011. 'NASPOT 11', a Sweetpotato Cultivar Bred by a Participatory Plant-breeding Approach in Uganda. HortScience. 46:317–321.

Nimmakayala, P., Vajja, G., and Reddy, U. K. 2011. *Ipomoea*. In *Wild Crop Relatives: Genomic and Breeding Resources*, C. Kole (Berlin: Springer), p. 123–132.

Pereira, G. da S., Gemenet, D. C., Mollinari, M., Olukolu, B. A., Wood, J. C., Diaz, F., et al. 2019. Multiple QTL mapping in autopolyploids: a random-effect model approach with application in a hexaploid sweetpotato full-sib population. bioRxiv. :622951.

Quesada-Ocampo, L. M. 2018. *Black Rot of Sweetpotato*. Raleigh, NC.: NC State Extension Publications. Available at: https://content.ces.ncsu.edu/black-rot-of-sweetpotato [Accessed January 21, 2020].

Quesada-Ocampo, L. M. 2016. *Emergency Section 18 Label Approved for Mertect to Control Black Rot Postharvest on Sweetpotato in North Carolina*.

Quesada-Ocampo, L. M., Al-Haddad, J., Scruggs, A. C., Buell, C. R., and Trail, F. 2016. Susceptibility of Maize to Stalk Rot Caused by *Fusarium graminearum* Deoxynivalenol and Zearalenone Mutants. Phytopathology. 106:920–927.

Quesada-Ocampo, L. M., and Hausbeck, M. K. 2010. Resistance in Tomato and Wild Relatives to Crown and Root Rot Caused by *Phytophthora capsici*. Phytopathology. 100:619–627.

R Core Team. 2019. *R: A language and environment for statistical computing*. Vienna, Austria: R Foundation for Statistical Computing. Available at: https://www.R-project.org/.

Revelle, W. R. 2017. psych: Procedures for Personality and Psychological Research. Available at: https://www.scholars.northwestern.edu/en/publications/psych-procedures-for-personality-and-psychological-research [Accessed October 21, 2020].

Santos, A. A., Lopes, K. V. G., Apfata, J. A. C., and Fontes, E. P. B. 2010. NSP-interacting kinase, NIK: a transducer of plant defence signalling. J. Exp. Bot. 61:3839–3845.

Schindelin, J., Arganda-Carreras, I., Frise, E., Kaynig, V., Longair, M., Pietzsch, T., et al. 2012. Fiji: an open-source platform for biological-image analysis. Nat. Methods. 9:676–682.

Scruggs, A. C., Basaiah, T., Adams, M. L., and Quesada-Ocampo, L. M. 2017. Genetic Diversity, Fungicide Sensitivity, and Host Resistance to *Ceratocystis fimbriata* Infecting Sweetpotato in North Carolina. Plant Dis. 101:994–1001.

Scruggs, A. C., and Quesada-Ocampo, L. M. 2016a. Cultural, chemical, and alternative control strategies for Rhizopus soft rot of sweetpotato. Plant Dis. 100:1532–1540.

Scruggs, A. C., and Quesada-Ocampo, L. M. 2016b. Etiology and Epidemiological Conditions Promoting Fusarium Root Rot in Sweetpotato. Phytopathology®. 106:909–919.

Sheikha, A., and Ray, R. C. 2015. Potential impacts of bioprocessing of sweet potato: Review. Crit. Rev. Food Sci. Nutr. 57:455–471.

Silva, J. L. S., Moura, E. F., Ilkiu-Borges, F., Galvão, J. R., Farias-Neto, J. T. de, Silva, G. B. da, et al. 2017. Morphoanatomy and histochemistry analyses of cassava roots do not discriminate resistant from susceptible genotypes to soft root rot. Acta Amaz. 47:1–6.

Stahr, M. N., Butler, S., Huerta, A. I., Ritchie, D. F., and Quesada-Ocampo, L. M. 2020. First Report of Bacterial Root Rot, Caused by *Dickeya dadantii*, on Sweetpotato (Ipomoea batatas) in North Carolina. Plant Dis. 104:2723–2723.

Stahr, M. N., and Quesada-Ocampo, L. M. 2019. Black Rot of Sweetpotato: A Comprehensive Diagnostic Guide. Plant Health Prog. 20:255–260.

Stahr, Madison, and Quesada-Ocampo, L. 2020. Effects of Water Temperature, Inoculum Concentration and Age, and Sanitizer Presence on Infection of *Ceratocystis fimbriata*, Causal Agent of Black Rot in Sweetpotato. Plant Dis. Available at: http://apsjournals.apsnet.org/doi/10.1094/PDIS-07-20-1475-RE [Accessed October 21, 2020].

Stahr, M., and Quesada-Ocampo, L. M. 2020. Assessing the Role of Temperature, Inoculum Density, and Wounding on Disease Progression of the Fungal Pathogen *Ceratocystis fimbriata* Causing Black Rot in Sweetpotato. Plant Dis. 104:930–937.

Tanaka, M. 2016. Recent Progress in Molecular Studies on Storage Root Formation in Sweetpotato (*Ipomoea batatas*). Jpn. Agric. Res. Q. JARQ. 50:293–299.

Tanaka, M., Takahata, Y., and Nakatani, M. 2005. Analysis of genes developmentally regulated during storage root formation of sweet potato. J. Plant Physiol. 162:91–102.

Tonn, N., and Greb, T. 2017. Radial plant growth. Curr. Biol. 27:878–882.

Torres, D. P., Proels, R. K., Schempp, H., and Hückelhoven, R. 2017. Silencing of RBOHF2 Causes Leaf Age–Dependent Accelerated Senescence, Salicylic Acid Accumulation, and Powdery Mildew Resistance in Barley. Mol. Plant. Microbe Interact. 30:906–918.

USDA. 2017. *National Nutrient Database for Standard Reference Release 28: Sweet potato*.

USDA. 2018. Secretary Perdue Issues USDA Statement on Plant Breeding Innovation ed. USDA Press.

USDA. 2016. *U.S. Specialty Crops Trade Issues*.

USDA-NASS. 2019. NC Sweetpotato harvested area and production measured in dollars.

Villordon, A. Q., Ginzberg, I., and Firon, N. 2014. Root architecture and root and tuber crop productivity. Trends Plant Sci. 19:419–425.

Wehner, T., and LaBonte, D. R. 2020. Sweetpotato, Lists 1-26 Combined.

Weimer, J. L., and Harter, L. L. 1921. Wound-cork Formation in the Sweet Potato. Jour Agr Res. 21:637–647.

Wickham, H., Chang, W., and Wickham, M. H. 2013. *Package "ggplot2."* Available at: http://ggplot2.org/.

Wu, S., Lau, K. H., Cao, Q., Hamilton, J. P., Sun, H., Zhou, C., et al. 2018. Genome sequences of two diploid wild relatives of cultivated sweetpotato reveal targets for genetic improvement. Nat. Commun. 9:1–12.

Zhang, H., Wang, C., Cheng, Y., Chen, X., Han, Q., Huang, L., et al. 2012. Histological and cytological characterization of adult plant resistance to wheat stripe rust. Plant Cell Rep. 31:2121–2137.

Zhao, J., Fu, J., Li, X., Xu, C., and Wang, S. 2009. Dissection of the factors affecting development-controlled and race-specific disease resistance conferred by leucine-rich repeat receptor kinase-type R genes in rice. Theor. Appl. Genet. 119:231–239.

Camilo H. Parada-Rojas et al. *Phytopathology* 28

TABLES

Table 1. Sweetpotato cultivars, advanced breeding lines, and wild relative accessions screened for their response to a North Carolina isolate AS236 of *Ceratocystis fimbriata* in root (R) and slip (S) experiments.

Accession	Cultivar	Taxonomy	Origin	Source	Exp.
PI 566610	AllGold	*Ipomoea batatas*	US	USDA-GRIN[a]	S
PI 566611	Apache	*Ipomoea batatas*	US	USDA-GRIN	S
Bayou Belle	Bayou Belle	*Ipomoea batatas*	US	MPRU[b]	R,S
PI 566613	Beauregard	*Ipomoea batatas*	US	MPRU	R,S
Bellevue	Bellevue	*Ipomoea batatas*	US	MPRU	R,S
Burgundy	Burgundy	*Ipomoea batatas*	US	MPRU	R,S
CIP 440168	Bwanjule	*Ipomoea batatas*	Uganda	NCSPB[c]	S
PI 628761	Carolina Ruby	*Ipomoea batatas*	US	MPRU	S
PI 606263	Chuanshu 27	*Ipomoea batatas*	China	USDA-GRIN	S
Covington	Covington	*Ipomoea batatas*	US	MPRU	R,S
CIP443752	Dimbuka Bukulula	*Ipomoea batatas*	Uganda	NCSPB	S
CIP443750	Ejumula	*Ipomoea batatas*	Uganda	NCSPB	S
Evangeline	Evangeline	*Ipomoea batatas*	US	MPRU	R,S
Hatteras	Hatteras	*Ipomoea batatas*	US	MPRU	R
PI 566632	Hernandez	*Ipomoea batatas*	US	MPRU	S
PI 566634	Hopi	*Ipomoea batatas*	US	USDA-GRIN	S
PI 573335	*I. littoralis*	*Ipomoea littoralis*	US	NCSPB	S
Japanese	Japanese	*Ipomoea batatas*	US	MPRU	S
PI 531122	Jewel	*Ipomoea batatas*	US	MPRU	R,S
PI 599390	Jishu5	*Ipomoea batatas*	China	USDA-GRIN	S
CIP100200.4	Kabode	*Ipomoea batatas*	Uganda	NCSPB	S
CIP441768	Kakamega 45879	*Ipomoea batatas*	Uganda	NCSPB	S
LSU-417	LSU-417	*Ipomoea batatas*	US	MPRU	S
Mahon	Mahon	*Ipomoea batatas*	US	MPRU	S
Murasaki	Murasaki	*Ipomoea batatas*	US	MPRU	R,S
PI 678406	NASPOT 10 O	*Ipomoea batatas*	Uganda	NCSPB	S
PI 681073	NASPOT 4	*Ipomoea batatas*	Uganda	NCSPB	S
NASPOT58	NASPOT 5	*Ipomoea batatas*	Uganda	NCSPB	S
PI 681075	NASPOT 8	*Ipomoea batatas*	Uganda	NCSPB	S
PI 681074	NASPOT 9 O	*Ipomoea batatas*	Uganda	NCSPB	S
NC04531	NC04531	*Ipomoea batatas*	US	MPRU	R,S
NC05198	Averre	*Ipomoea batatas*	US	MPRU	R,S
CIP441745	New Kawogo	*Ipomoea batatas*	Uganda	NCSPB	S
PI 153905	Norin No.2	*Ipomoea batatas*	Japan	USDA-GRIN	S
PI 153907	Norin No.4	*Ipomoea batatas*	Japan	USDA-GRIN	S
Norton	Norton	*Ipomoea batatas*	US	MPRU	S
NCNSP0306	NSP306	*Ipomoea trifida*	Colombia	NCSPB	S
O'Henry	O'Henry	*Ipomoea batatas*	US	MPRU	R,S

NCNSP0323	NSP323	*Ipomoea triloba*	Mexico	NCSPB	S
Orleans	Orleans	*Ipomoea batatas*	US	MPRU	R,S
PI 566646	Porto Rico	*Ipomoea batatas*	US	MPRU	R,S
NC413	Stokes Purple	*Ipomoea batatas*	US	MPRU	R,S
PI 566656	Sunnyside	*Ipomoea batatas*	US	USDA-GRIN	S
Tanzania	Tanzania	*Ipomoea batatas*	Uganda	NCSPB	S
CIP100201	Tomulabula	*Ipomoea batatas*	Uganda	NCSPB	S
PI 566660	Travis	*Ipomoea batatas*	US	MPRU	S
PI 681074	VitA NASPOT 9 O	*Ipomoea batatas*	Uganda	NCSPB	S
Bonita	White Bonita	*Ipomoea batatas*	US	MPRU	R,S

[a] United States Department of Agriculture - Germplasm Resources Information Network
[b] Micropropagation and Repository Unit
[c] North Carolina Sweetpotato Breeding and Genetics Program

Table 2. Storage root susceptibility of 16 sweetpotato cultivars and advanced breeding lines to *Ceratocystis fimbriata* isolate AS236.

Cultivar	AUDPC [u]	CLR [v]	Cultivar rankings			d [y]
			a	*b*	*c*	
Jewel	25.20 de	0.08 g [z]	2	1	3	-3.68
Covington	23.44 e	0.09 fg	1	2	3	-3.68
NC04531	29.32 abcd	0.10 efg	7	5	12	-1.30
O'Henry	27.06 cde	0.13 cdef	4	8	12	-1.30
Beauregard	30.65 abc	0.09 fg	10	3	13	-1.04
Murasaki	26.85 cde	0.15 bcde	3	10	13	-1.04
Orleans	31.44 abc	0.09 fg	12	4	16	-0.25
Evangeline	27.78 bcde	0.16 bcd	5	11	16	-0.25
Bayou Belle	30.88 abc	0.10 defg	11	6	17	0.02
Porto Rico	29.09 abcd	0.17 abc	6	14	20	0.81
Averre	32.13 abc	0.13 cdef	14	7	21	1.07
Burgundy	30.32 abcd	0.17 bc	9	12	21	1.07
Stokes Purple	29.81 abcd	0.22 ab	8	15	23	1.60
Hatteras	33.77 a	0.14 bcdef	16	9	25	2.13
Bellevue	32.46 ab	0.17 bc	15	12	27	2.66
White Bonita	31.90 abc	0.28 a	13	16	29	3.18
					16.94 [w]	

[u] Area under the disease progress curve (AUDPC) calculated from surface lesion diameter measurements recorded over a 24-day period.

[v] Cross-sectional lesion ratio (CLR) calculated 24 days post-inoculation using the image analysis software Fiji.

[w] Grand mean of the rank-sums (G); *a:* cultivar ranking based on AUDPC means; *b:* cultivar ranking based on CLR means; *c* = Rank-sum (*a* + *b*) for each cultivar; *d:* deviation from the grand mean (G) of the rank-sums [(*d* = (*c* − G)/standard deviation) x 2].

[y] Colors of deviations denote the level of susceptibility with deviations close to -4 indicating lower susceptibility and deviations close +4 indicating higher susceptibility

[z] Means followed by the same letter are not significantly different according to Tukey-Kramer test ($\alpha = 0.05$).

Table 3. Above and below ground incidence of 47 sweetpotato cultivars, advanced breeding lines, and wild relative accessions used in the slip experiment to screen for resistance against *Ceratocystis fimbriata.*

Accessions	Cultivar	Disease incidence (%)^x	
		Above ground ^{y}	Below ground ^{z}
PI 681075	NASPOT 8	3.39 ijk	97.50 a
PI 566656	Sunnyside	35.86 a-f	97.50 a
LSU-417	LSU-417	2.31 jk	97.50 a
PI 566660	Travis	52.98 a-d	95.30 ab
NCNSP0306	NCNSP0306	27.47 a-i	95.00 abc
CIP443750	Ejumula	57.61 a-d	95.00 abc
PI 681074	NASPOT 9 O	31.78 a-f	94.40 a-d
Bayou Belle	Bayou Belle	18.14 c-k	93.90 a-d
CIP100201	Tomulabula	27.07 a-i	93.30 a-e
CIP441745	New Kawogo	3.39 ijk	83.40 a-f
PI 566634	Hopi	3.57 h-k	83.40 a-f
PI 628761	Carolina Ruby	38.11 a-f	82.00 a-f
White Bonita	White Bonita	3.39 ijk	82.00 a-f
PI 566646	Porto Rico	16.03 d-k	79.70 a-g
Japanese	Japanese	72.53 a	77.10 a-g
Bellevue	Bellevue	3.39 ijk	77.00 a-g
NC_413	Stokes Purple	50 a-d	74.20 b-g
PI 606263	Chuanshu 27	3.93 g-k	73.60 b-g
PI 153905	Norin No.2	25.98 a-i	72.10 b-h
CIP 440168	Bwanjule	6.47 f-k	70.10 b-h
NASPOT 5	NASPOT 5	7.06 e-k	69.90 b-h
Mahon	Mahon	18.14 c-k	68.30 b-h
NCNSP0323	NSP323	1.73 k	66.60 b-h
CIP441768	Kakamega 45879	28.18 a-i	65.80 b-h
NC05198	Averre	3.57 h-k	65.80 b-h
PI 595887	Tanzania	24.28 b-i	65.80 b-h
PI 678406	NASPOT 10 O	1.73 k	63.90 b-h
NC04531	NC04531	19.71 c-j	63.70 b-h
O'Henry	O'Henry	6.47 f-k	63.20 b-h
CIP100200.4	Kabode	1.73 k	61.80 c-h
PI 566610	AllGold	31.33 a-g	61.70 d-h
PI 153907	Norin No.4	68.67 ba	57.50 e-h
PI 681073	NASPOT 4	19.71 c-j	56.80 e-h

Camilo H. Parada-Rojas et al. *Phytopathology* 32

PI 599390	Jishu5	7.06 e-k	55.30 fgh
PI 531122	Jewel	62.08 abc	53.90 fgh
Murasaki	Murasaki	42.39 a-e	52.40 fgh
Evangeline	Evangeline	18.62 c-k	52.20 fgh
Norton	Norton	3.39 ijk	50.00 fgh
PI 566611	Apache	3.57 h-k	50.00 fgh
CIP443752	Dimbuka Bukulula	3.93 g-k	50.00 fgh
PI 566613	Beauregard	1.73 k	45.60 fgh
Covington	Covington	6.47 f-k	40.90 fgh
PI 566632	Hernandez	1.73 k	38.80 fgh
PI 681074	VitA NASPOT 9 O	3.39 ijk	36.30 fgh
Orleans	Orleans	2.31 jk	36.30 fgh
PI 573335	*I. littoralis*	29.36 a-h	32.10 gh
Burgundy	Burgundy	1.73 k	22.90 h

[x] Disease incidence percentage within a column for each cultivar followed by the same letter are not significantly different ($P = 0.05$).

[y] Mean incidence of above ground symptomatic tissue. Examples of symptoms are included in Figure. 1S

[z] Mean incidence of below ground symptomatic tissue. Examples of symptoms are included in Figure. 3

FIGURE LEGENDS

Fig. 1. Cross-section image taken from **A.** Jewel, **B.** Covington, **C.** Burgundy, and **D.** White Bonita sweetpotatoes at 24 days post inoculation with *Ceratocystis fimbriata* isolate AS236. Dark brown areas constitute the pattern of necrosis after infection. Note the distinctive constrained necrotic area in Jewel and Covington in contrast with the extended area in Burgundy and White Bonita.

Fig. 2. Surface lesion diameter progression over 24 days for Jewel, Covington, Burgundy, and White Bonita sweetpotatoes inoculated with *Ceratocystis fimbriata* isolate AS236. Data were analyzed in R using the *glmmTMB* function from the R package glmmTMB. Lesion diameter was significantly smaller in cultivars Jewel and Covington after 4 days post inoculation and remained significant for the duration of the experiment ($P = 0.019$).

Fig. 3. Response of sweetpotato cultivars Burgundy, Averre, and Sunnyside at 42 days post inoculation with *Ceratocystis fimbriata* isolate AS236. Red circles denote crown necrotic lesions. White pushing pins denote plants deceased before root washing.

Fig. 4. Response of Covington sweetpotato roots of different total cross-section area to inoculation with *Ceratocystis fimbriata* isolate AS236. Photograph was taken 24 days post-inoculation (dpi). Notice constrained necrotic lesion area on root with greater total cross-sectional area. Blue ruler indicates metric scale. All roots were harvested at the same time, from the same field, and same clone.

Fig. 5. Cross-sectional lesion ratio (CLR) and total cross-sectional area of Covington sweetpotato roots inoculated with *Ceratocystis fimbriata* isolate AS236. Measurements were recorded 24 days post-inoculation. (Spearman's r = -0.77; $P < 0.0001$).

Fig. 1S. Above ground symptoms of cultivar Norin 2 observed at 13 days post inoculation with *Ceratocystis fimbriata* isolate AS236. Pink arrows denote cracking of stems and wilting of slips.

Fig. 2S. Lesion diameter of *Ceratocystis fimbriata* isolate AS236 on Covington roots with different total cross-section area. Measurements were recorded 24 days post-inoculation. Predicted line was fitted using a linear model ($R^2 = 0.01$; $P = 0.105$). All roots were harvested at the same time, from the same field, and same clone.
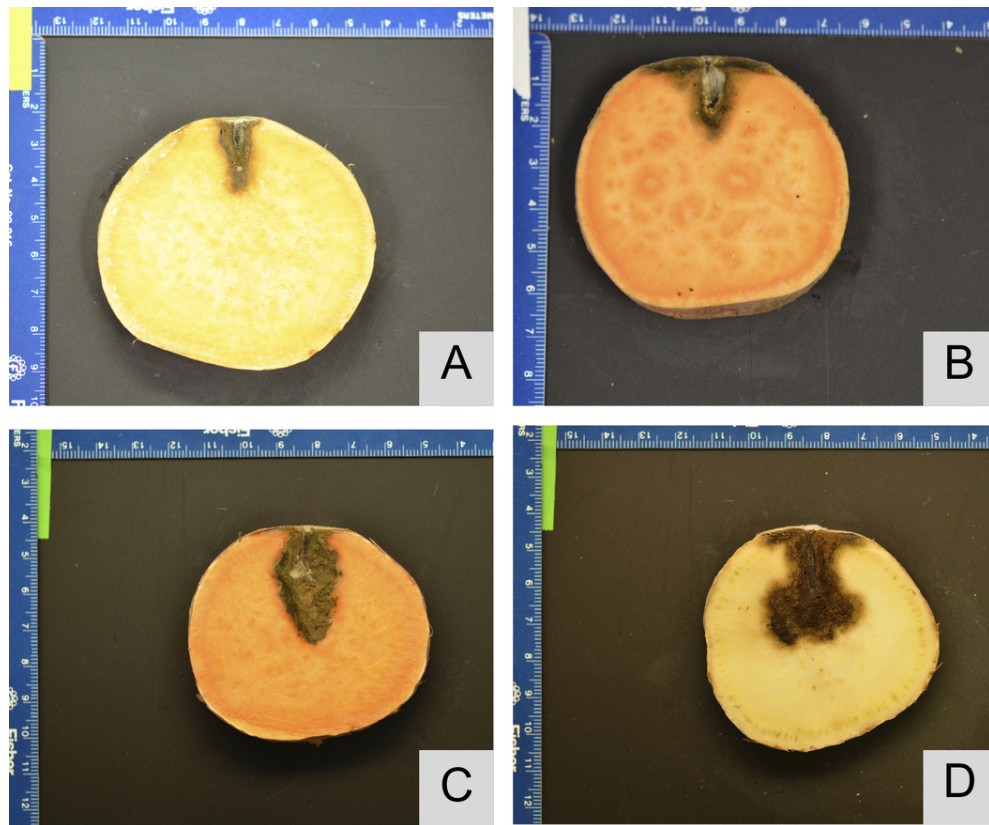
Fig. 1. Cross-section image taken from **A.** Jewel, **B.** Covington, **C.** Burgundy, and **D.** White Bonita sweetpotatoes at 24 days post inoculation with *Ceratocystis fimbriata* isolate AS236. Dark brown areas constitute the pattern of necrosis after infection. Note the distinctive constrained necrotic area in Jewel and Covington in contrast with the extended area in Burgundy and White Bonita.

90x75mm (300 x 300 DPI)
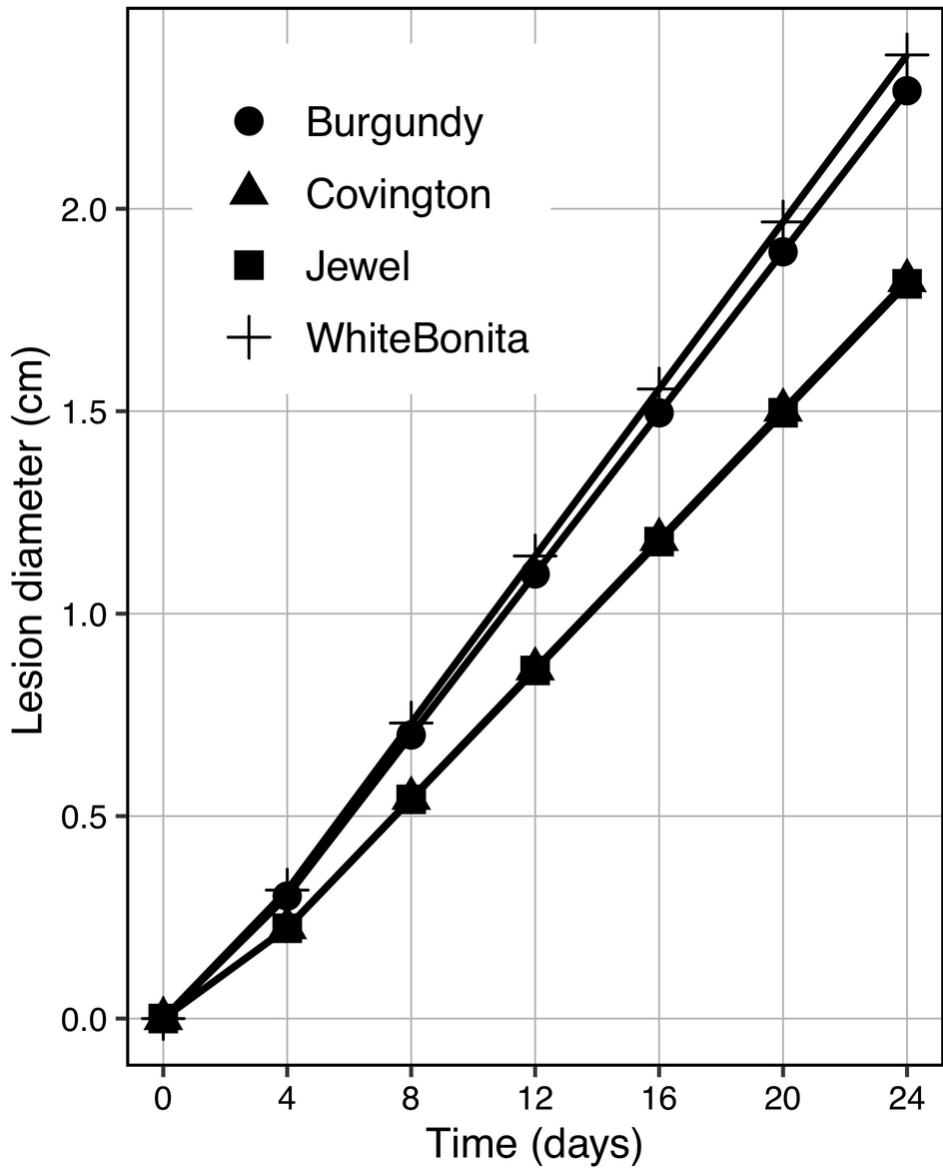
Fig. 2. Surface lesion diameter progression over 24 days for Jewel, Covington, Burgundy, and White Bonita sweetpotatoes inoculated with *Ceratocystis fimbriata* isolate AS236. Data were analyzed in R using the glmmTMB function from the R package *glmmTMB*. Lesion diameter was significantly smaller in cultivars Jewel and Covington after 4 days post inoculation and remained significant for the duration of the experiment ($P = 0.019$).

82x101mm (300 x 300 DPI)

Fig. 3. Response of sweetpotato cultivars Burgundy, Averre, and Sunnyside at 42 days post inoculation with *Ceratocystis fimbriata* isolate AS236. Red circles denote crown necrotic lesions. White pushing pins denote plants deceased before root washing.

106x195mm (300 x 300 DPI)
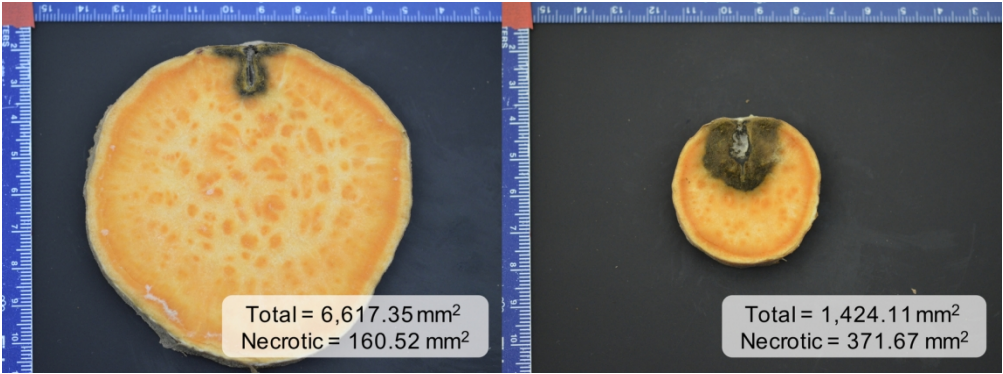
Fig. 4. Response of Covington sweetpotato roots of different total cross-section area to inoculation with *Ceratocystis fimbriata* isolate AS236. Photograph was taken 24 days post-inoculation (dpi). Notice constrained necrotic lesion area on root with greater total cross-sectional area. Blue ruler indicates metric scale. All roots were harvested at the same time, from the same field, and same clone.

158x58mm (300 x 300 DPI)
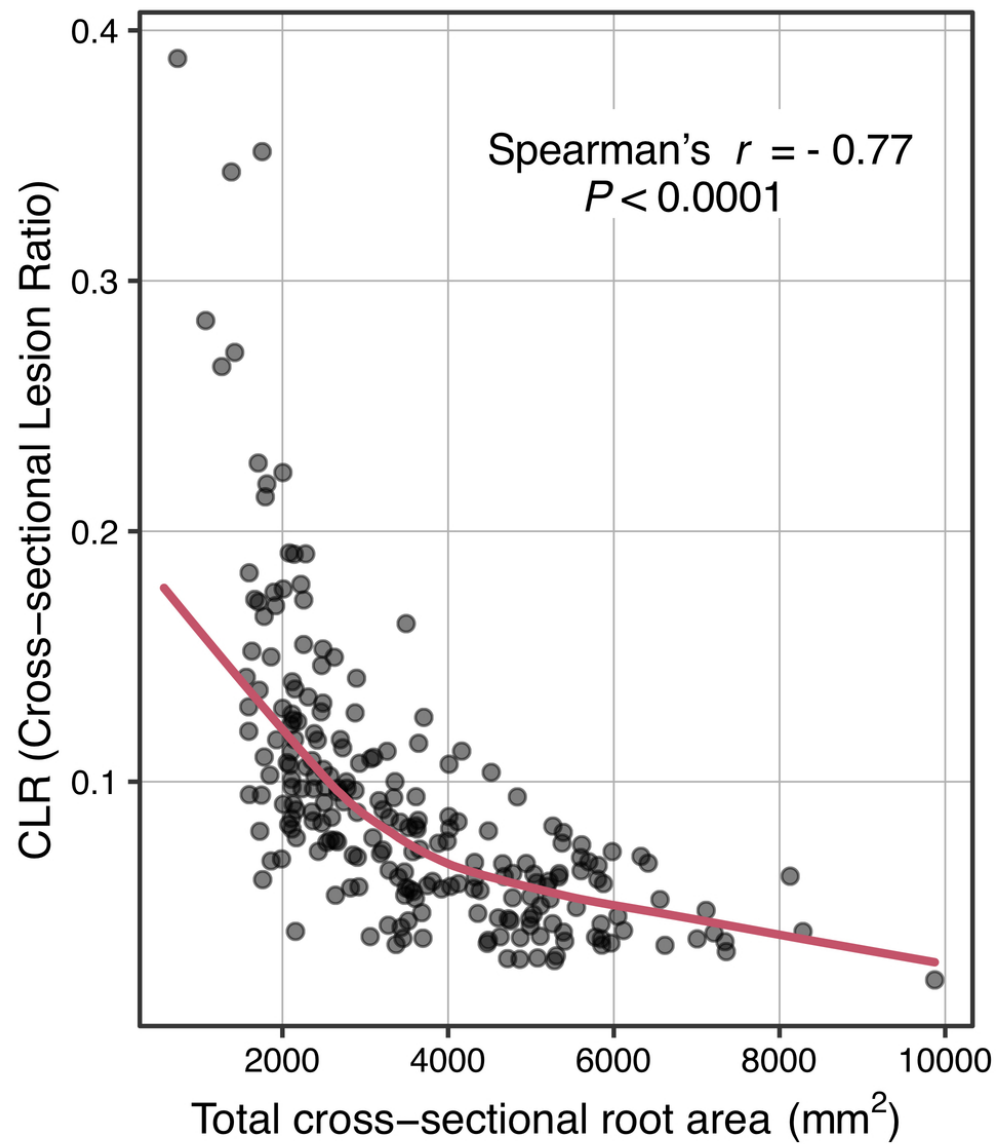
Fig. 5. Cross-sectional lesion ratio (CLR) and total cross-sectional area of Covington sweetpotato roots inoculated with *Ceratocystis fimbriata* isolate AS236. Measurements were recorded 24 days post-inoculation. (Spearman's r = -0.77; P < 0.0001).
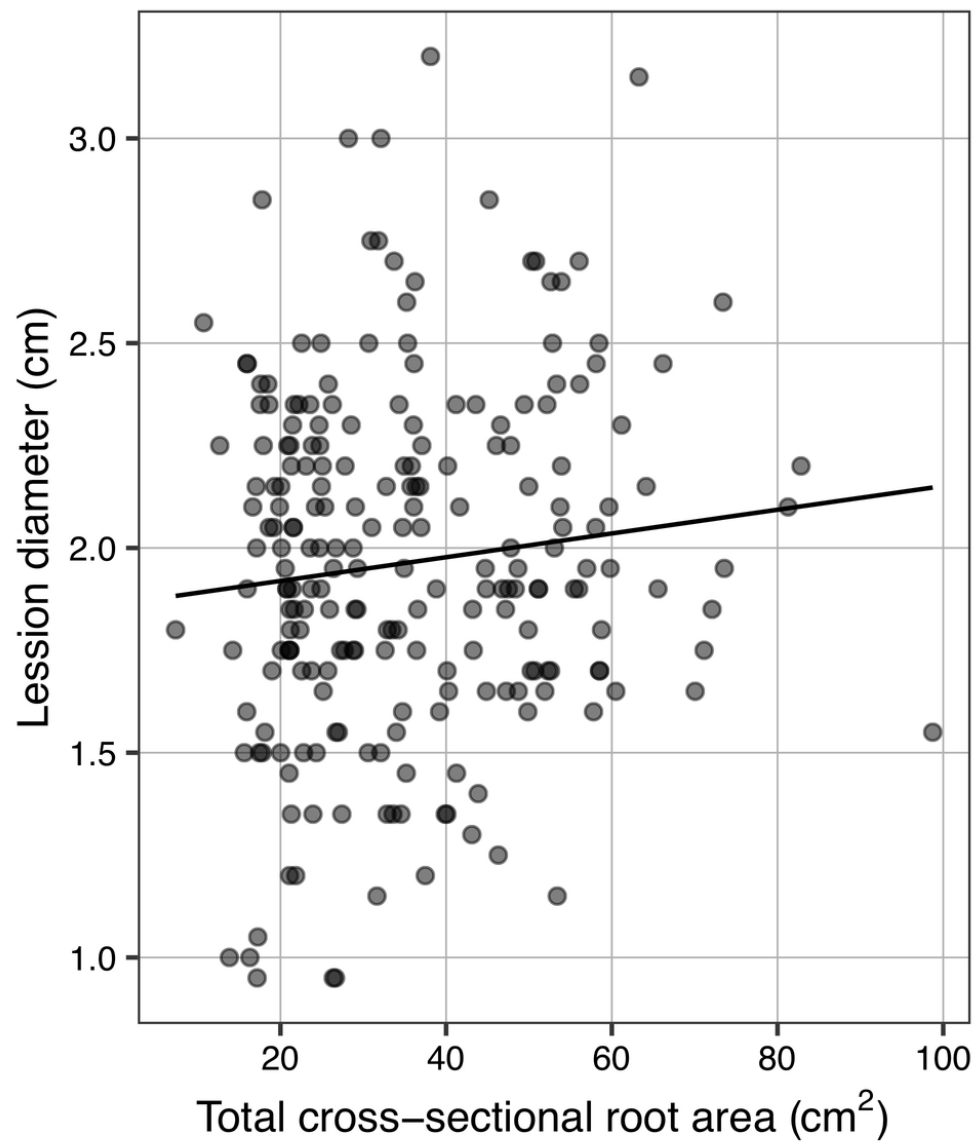
82x97mm (300 x 300 DPI)

Fig. 1S. Above ground symptoms of cultivar Norin 2 observed at 13 days post inoculation with *Ceratocystis fimbriata* isolate AS236. Pink arrows denote cracking of stems and wilting of slips.

88x45mm (300 x 300 DPI)

Fig. 2S. Lesion diameter of *Ceratocystis fimbriata* isolate AS236 on Covington roots with different total cross-section area. Measurements were recorded 24 days post-inoculation. Predicted line was fitted using a linear model (R^2 = 0.01; P = 0.105). All roots were harvested at the same time, from the same field, and same clone.

82x97mm (300 x 300 DPI)